This is an open access article published under an ACS AuthorChoice License, which permits copying and redistribution of the article or any adaptations for non-commercial purposes.

ACS OMEGA

http://pubs.acs.org/journal/acsodf

Article

UPLC/MS/MS-Based Metabolomics Study of the Hepatotoxicity and Nephrotoxicity in Rats Induced by *Polygonum multiflorum* Thunb.

Yan Yan,[#] Ning Shi,[#] Xuyang Han, Guodong Li, Binyu Wen,* and Jian Gao*

Cite This: *ACS Omega* 2020, 5, 10489−10500

Read Online

ACCESS | Metrics & More | Article Recommendations | Supporting Information

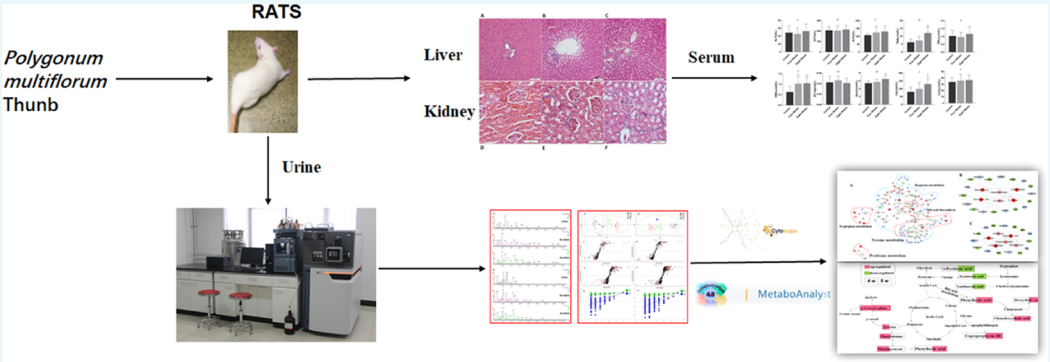

ABSTRACT: *Polygonum multiflorum* Thunb. (PM) is one of the most frequently used natural products in China. Its hepatotoxicity has been proven and reported. However, chronic PM toxicity is a dynamic process, and a few studies have reported the long-term hepatotoxic mechanism of PM or its nephrotoxicity. To elucidate the mechanism of hepatotoxicity and nephrotoxicity induced by PM after different administration times, different samples from rats were systematically investigated by traditional biochemical analysis, histopathological observation, and nontargeted metabolomics. The concentrations of direct bilirubin (DBIL) at 4 weeks and total bile acid, DBIL, uric acid, and blood urea nitrogen at 8 weeks were significantly increased in the treatment group compared with those in the control group. Approximately, 12 metabolites and 24 proteins were considered as unique toxic biomarkers and targets. Metabolic pathway analysis showed that the primary pathways disrupted by PM were phenylalanine and tyrosine metabolism, which resulted in liver injury, accompanied by chronic kidney injury. As the administration time increased, the toxicity of PM gradually affected vitamin B6, bile acid, and bilirubin metabolism, leading to aggravated liver injury, abnormal biochemical indicators, and marked nephrotoxicity. Our results suggest that the hepatotoxicity and nephrotoxicity caused by PM are both dynamic processes that affect different metabolic pathways at different administration times, which indicated that PM-induced liver and kidney injury should be treated differently in the clinic according to the degree of injury.

INTRODUCTION

Polygonum multiflorum Thunb. (PM), which is called Heshouwu in China, is the most commonly used medicinal plant in Asia.[1] Many ingredients are found in this plant, including anthraquinones, stilbene glycosides, phospholipids, phenols, flavonoids, etc.[2,3] The most important biologically active components of PM are quinones that have antimicrobial, antidiarrhea, antihypertensive, and anticancer properties and diverse prospects.[4−7] However, it was reported that PM caused serious adverse effects, especially hepatotoxicity.[8] Current clinical reports suggested that the long-term administration of PM may cause irreversible liver damage, which is characterized by cholestasis. Therefore, the evaluation of the safety of PM is particularly urgent and important.[9,10] Several studies have reported the hepatotoxicity and mechanism of PM. For example, some studies have focused on the harvesting times of PM,[11] performed high-throughput screening assays to study the hepatotoxicity mechanisms of PM,[12] and evaluated cytochrome P450 enzyme activity after PM administration.[13] Dong et al. showed that the long-term administration of PM led to a certain degree of renal damage.[14] However, the mechanism of hepatotoxicity induced by PM is still unclear and worthy of further exploration. In addition, most studies on the toxicity of PM have focused on liver injury, but a few have focused on the nephrotoxicity induced by PM. The correlation analysis of chemical constituents in *Rheum officinale* with hepatorenal toxicity suggested that both free and bound

Received: February 12, 2020
Accepted: April 3, 2020
Published: April 28, 2020

© 2020 American Chemical Society

https://dx.doi.org/10.1021/acsomega.0c00647
ACS Omega 2020, 5, 10489−10500

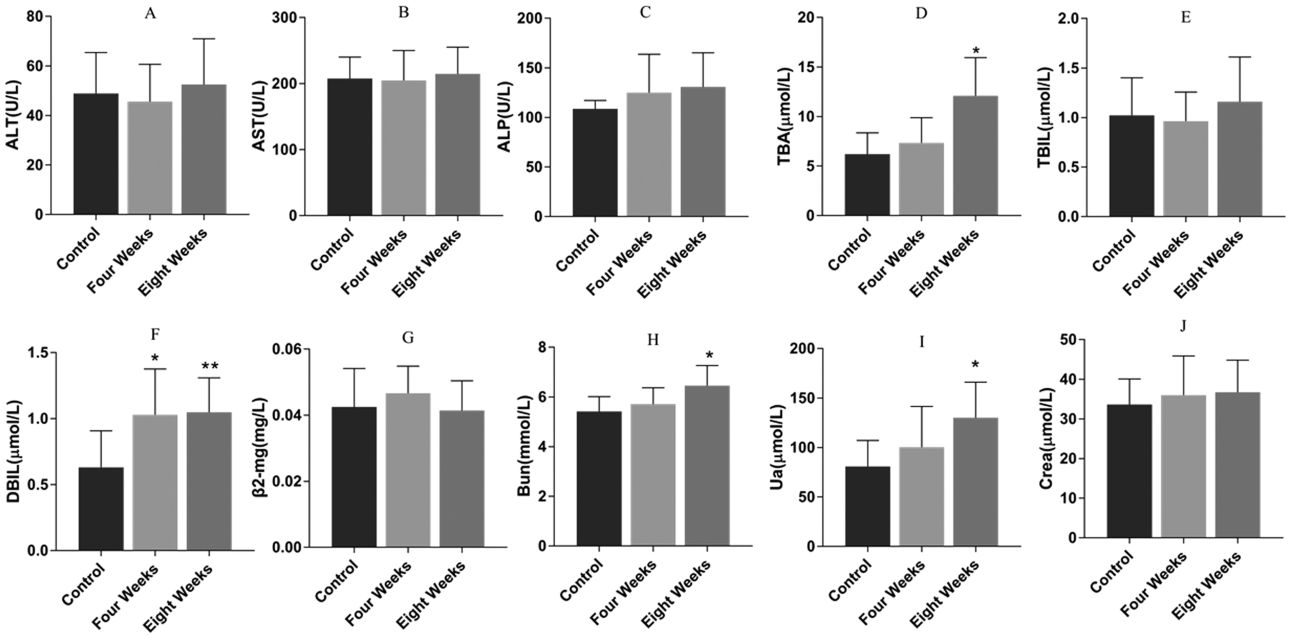

Figure 1. Serum levels of ALT (A), AST (B), ALP (C), TBA (D), TBIL (E), DBIL (F), β2-MG (G), BUN (H), UA (I), and Crea (J) (n = 10). Data were expressed as the mean ± standard deviation (SD) and were analyzed by analysis of variance (ANOVA). *p < 0.05 vs control group; **p < 0.01 vs control group. (A)−(F) Index of the liver and (G)−(J) index of the kidney.

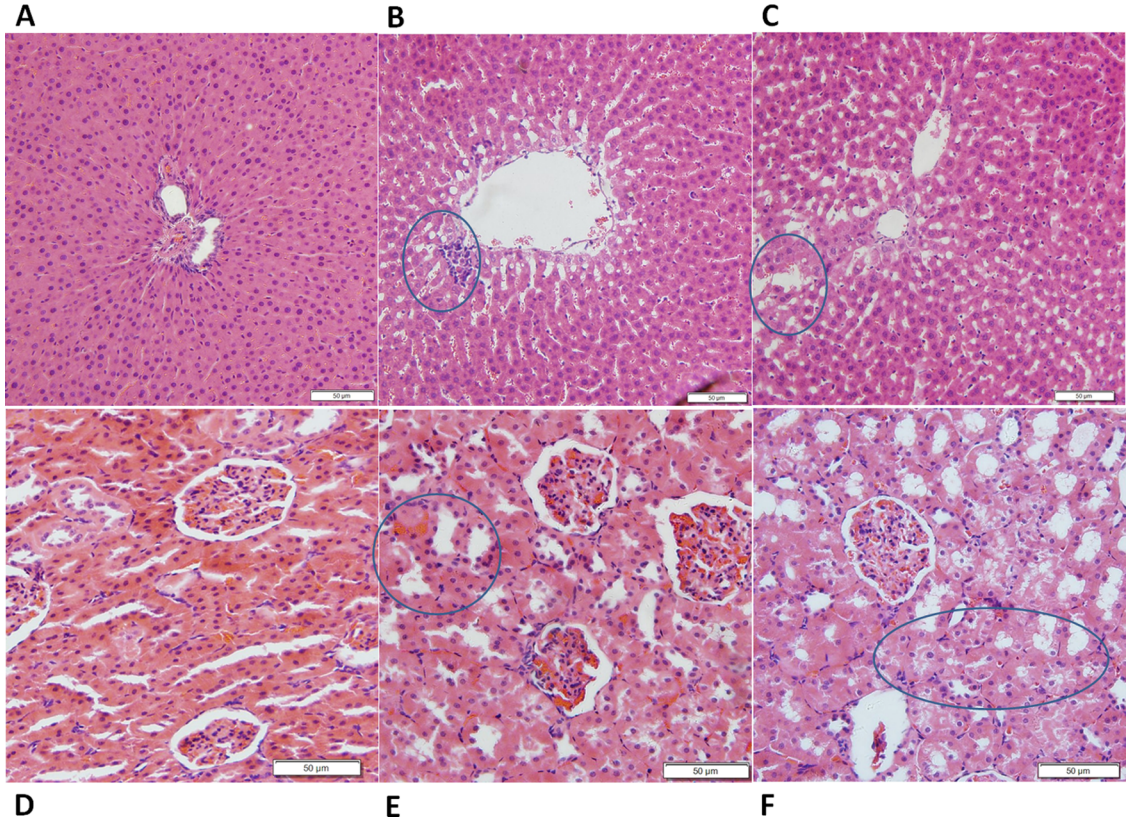

Figure 2. Liver and kidney histopathology in three groups (n = 5). Histological sections were stained with hematoxylin and eosin (H&E) (200× magnification). The liver tissues from three groups (control group, PM group I, and PM group II) are shown in (A), (B), and (C), respectively. (B) Hepatic sinusoids were dilated, and there was no obvious focal aggregation of inflammatory cells. The arrangement of hepatocytes was basically normal. (C) Cell shrinkage appeared with a disordered cord arrangement. Kary pyknosis was detected with blurred structures, and the edges were unclear. Kidney tissues from three groups (control group, PM group I, and PM group II) are shown in (D), (E), and (F), respectively. (E) Kidney structure was clear and the glomerular structure was normal, but the proximal convoluted tubules were edematous and degenerated. (F) Edema and degeneration of the proximal convoluted tubules were observed in the renal interstitium.

https://dx.doi.org/10.1021/acsomega.0c00647
ACS Omega 2020, 5, 10489−10500

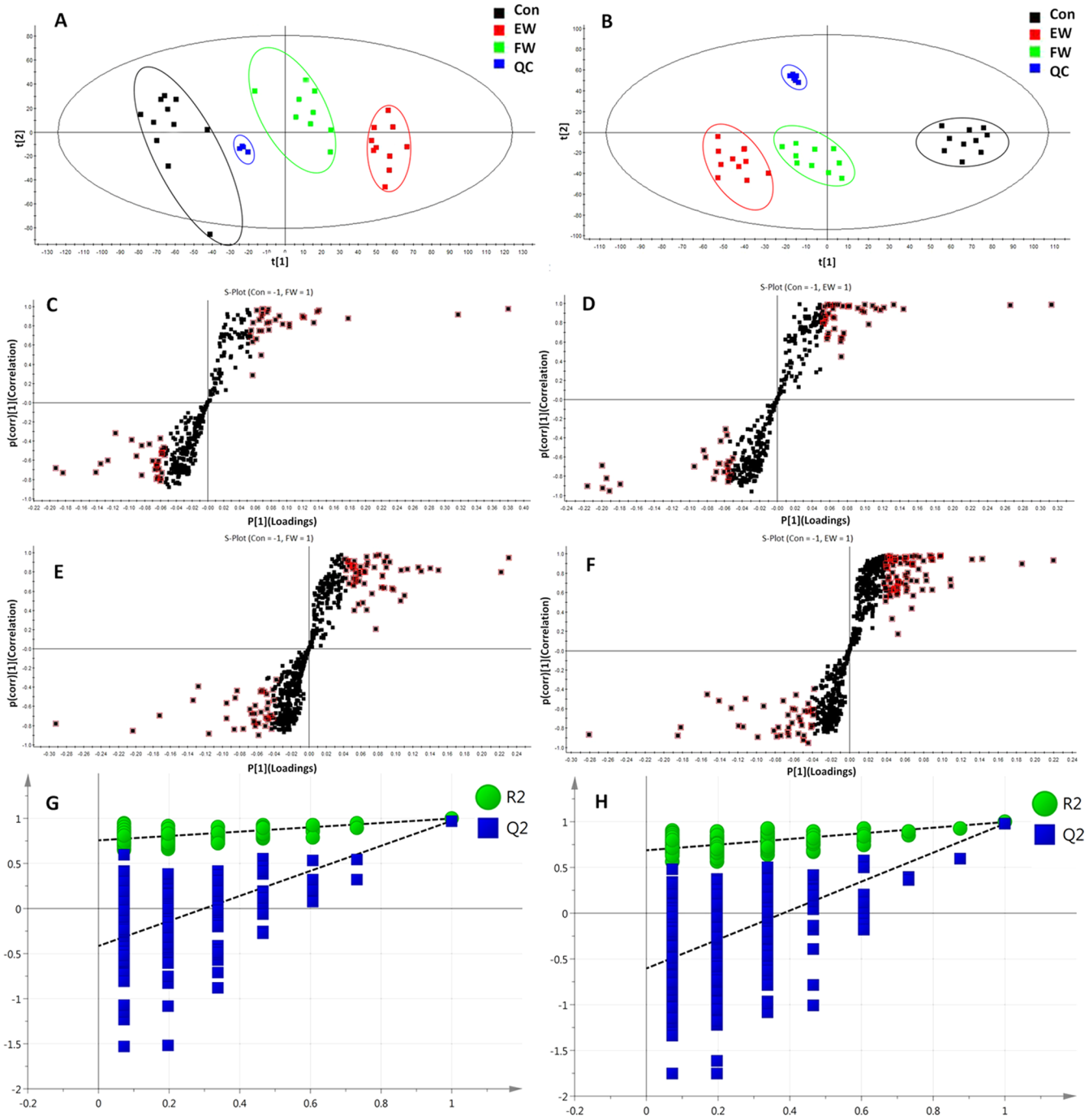

Figure 3. PCA and orthogonal projections to latent structures discriminant analysis (OPLS-DA) plots of PM groups in ESI$^+$ and ESI$^-$ modes, respectively. PCA plots of control and PM groups in ESI$^+$ (A) and ESI$^-$ (B) modes. *S*-plot of OPLS-DA for control group versus PM groups (I and II) in ESI$^+$ (C, D) and ESI$^-$ (E, F) modes. Metabolites with variables with importance parameter (VIP) >1 were marked with a red square in ESI$^+$ (C, D) and ESI$^-$ (E, F). Cross-validated score plots (G, H) (n = 10).

anthraquinones may have nephrotoxicity.[15] Therefore, current studies on the nephrotoxicity of PM are insufficient.

Metabolomics has been widely used to study the pharmacological and toxicological mechanisms of traditional Chinese medicine. Wide dynamic range and chemical diversity coverage are the main advantages of liquid chromatography–mass spectrometry (LC/MS), which is very suitable for nontargeted metabolomics study.[16−18] At present, there were some preliminary reports on PM hepatotoxicity; for example, Dong et al. reported that the hepatotoxicity of PM primarily impacted nine types of bile acid;[19] Li et al. investigated the effect of different PM extracts on idiosyncratic drug-induced liver injury.[20] Additionally, rat urine and serum samples have been analyzed using metabolomics techniques, and some metabolic pathways were found to be involved in the hepatotoxicity of PM, including the tricarboxylic acid cycle, amino acid metabolism, and vitamin B6 metabolism.[21] However, different administration times of PM may produce different toxic effects, especially with prolonged exposure time, and the toxicological mechanisms of some components may change constantly.[22] It is the toxicity of PM that is a chronic

https://dx.doi.org/10.1021/acsomega.0c00647
ACS Omega 2020, 5, 10489−10500

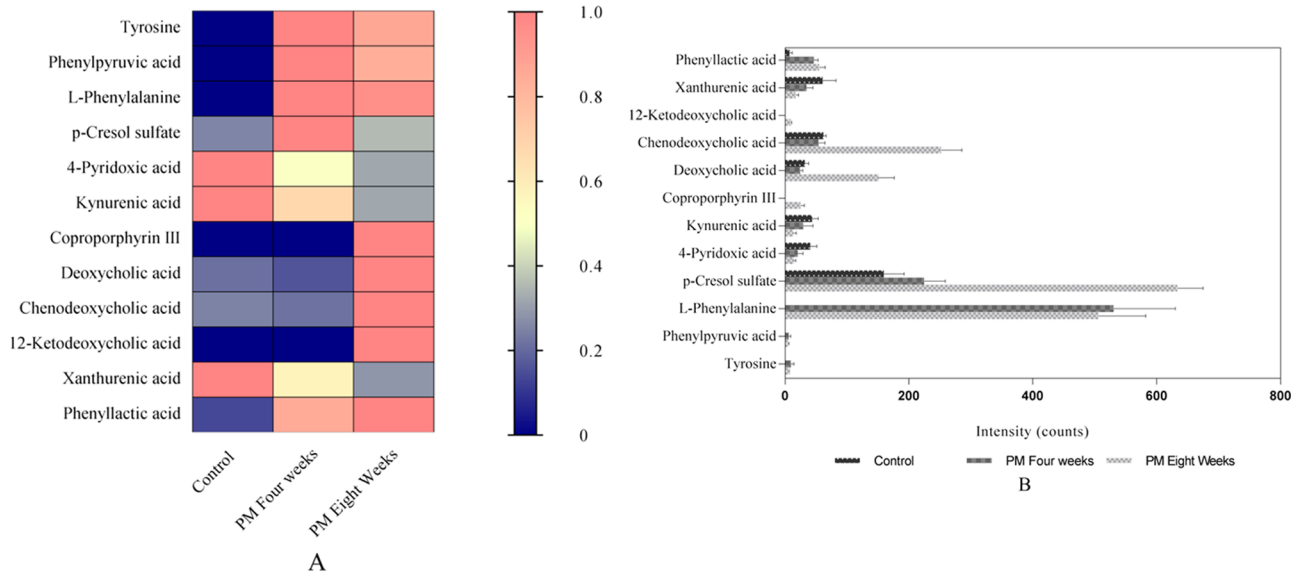

Figure 4. (A) Heat map showing the discriminatory capacity of each metabolite estimated. Colors correspond to average normalized quantities; red and blue represent high and low values, respectively. (B) Concentration changes of potential biomarkers in the control and two different stages of PM groups.

and changing process, and a few studies have reported its toxicity mechanism at different exposure durations.

In summary, serum, liver, kidney, and urine samples from rats were systematically investigated in this study by biochemical analysis, pathological observation, and non-targeted metabolomics to evaluate the toxicity of PM at different times of administration. The metabolic profiles of urine samples from PM-treated and untreated rats were analyzed to screen potential biomarkers of liver and kidney damage. Then, the metabolic pathways and metabolites that correlated with protein targets were explored by combining the biochemical indices and metabolic markers to clarify liver and kidney injury mechanisms of PM.

RESULTS

Biochemical Analysis. The results of the biochemical analysis are shown in Figure 1A–J. Both the concentrations of direct bilirubin (DBIL) in PM group I and total bile acids (TBAs), DBIL, urine acid (UA), and blood urea nitrogen (BUN) in PM group II were significantly increased compared with those in the control group ($p < 0.05$ or 0.01). However, other biochemical indices, such as serum alanine aminotransferase (ALT), aspartate aminotransferase (AST), alkaline phosphatase (ALP), TBIL, and creatinine (Crea) increased slightly in the PM groups with no significant differences.

Histopathological Observations. The histopathological analysis of the hepatic and renal tissues was performed to evaluate tissue damage due to PM exposure. Regular spongy hepatic plates were observed in the liver tissues of the control group and radiated regularly around the terminal hepatic veins (Figure 2A). The nuclei were centered, round, and contained one or more nucleoli. After the administration of PM for 4 weeks (Figure 2B), the hepatic sinusoids were dilated and there was no obvious focal aggregation of inflammatory cells. The arrangement of hepatocytes was basically normal. After the administration of PM for 8 weeks (Figure 2C), cell shrinkage appeared with a disordered cord arrangement. Kary pyknosis was detected with blurred structures, and the edges were unclear. The hepatocellular cytopathic effect was more severe at the longer PM administration period.

For the kidney tissue, the normal renal tissue structure was clear and the glomerular structure was normal in the control group (Figure 2D). There was no obvious pathological change. After the administration of PM for 4 weeks (Figure 2E), the kidney structure was clear and the glomerular structure was normal, but the proximal convoluted tubules were edematous and degenerated. After the administration of PM for 8 weeks (Figure 2F), edema and degeneration of the proximal convoluted tubules were observed in the renal interstitium. Pathological results showed that the renal injury was aggravated by the prolonged administration of PM.

Multivariate Statistical Analysis and Potential Biomarkers. Urinary chromatography was performed by ultra-performance liquid chromatography–quadrupole-time-of-flight mass spectrometry (UPLC/Q-TOF-MS) in both positive- and negative-ion modes. To identify differences in metabolic components among the three groups, multivariate statistical analysis was used to investigate the metabolites (see Figure S2 in the Supporting Information for the comprehensive analysis of the positive and negative ions in the urine samples).

After peak matching, all of the variables in the control group and PM groups were analyzed by principal component analysis (PCA). The positive and negative mode plots of urinary samples are shown in Figure 3A,B. There was an obvious separation trend between the control and PM groups in both positive and negative modes. An anomalous sample was removed in the clustering of data, and the positive and negative mode plots are shown in Figure 3A,B. Figure 3A,B shows the obvious separation among the three groups. The samples from the control group clustered together and remained relatively far from those from the PM groups. In addition, the two PM groups with different administration times remained relatively far from each other, as shown in Figure 3A,B. The results suggested that there were considerable metabolite differences between the control and PM groups. The significant metabolic differences among the three groups indicated that further

https://dx.doi.org/10.1021/acsomega.0c00647
ACS Omega 2020, 5, 10489–10500

Table 1. Identification of Potential Biomarkers[c,d]

no.	retention time (min)	mass-to-charge ratio	type	identified compound	comparison between groups (fold change)
1	0.79	182.0467	$[M - H]^-$	4-pyridoxic acid[a]	Con/EW (2.8)
2	0.84	204.0638	$[M + Na]^+$	L-tyrosine[a,b]	Con/FW (<1)
3	1.28	204.0310	$[M - H]^-$	xanthurenic acid[a]	Con/EW (3.5)
4	1.58	188.0362	$[M - H]^-$	kynurenic acid[a,b]	Con/EW (3.1)
5	1.70	163.0405	$[M - H]^-$	phenylpyruvic acid[a]	Con/FW (<1)
6	1.85	188.0688	$[M + Na]^+$	L-phenylalanine[a,b]	Con/FW (<1)
7	2.97	187.0075	$[M - H]^-$	*p*-cresol sulfate[a]	Con/FW (2.8), Con/EW (4.0)
8	3.37	165.0564	$[M - H]^-$	phenyllactic acid[a]	Con/EW (6.2)
9	8.33	391.2852	$[M + H]^+$	12-ketodeoxycholic acid[a]	Con/EW (<1)
10	8.44	655.2765	$[M + H]^+$	coproporphyrin III[a]	Con/EW (<1)
11	11.65	391.2875	$[M - H]^-$	chenodeoxycholic acid[a,b]	Con/EW (<1)
12	11.92	391.2868	$[M - H]^-$	deoxycholic acid[a,b]	Con/EW (<1)

[a]Metabolites confirmed by literature or database searches and mass spectrometry (MS) fragmentation. [b]Metabolites confirmed using standard compounds. [c]Con-FW: significant differences in metabolites with $p < 0.05$ between the control and PM group I (4 weeks). [d]Con-EW: significant differences in metabolites with $p < 0.05$ between the control and PM group II (8 weeks).

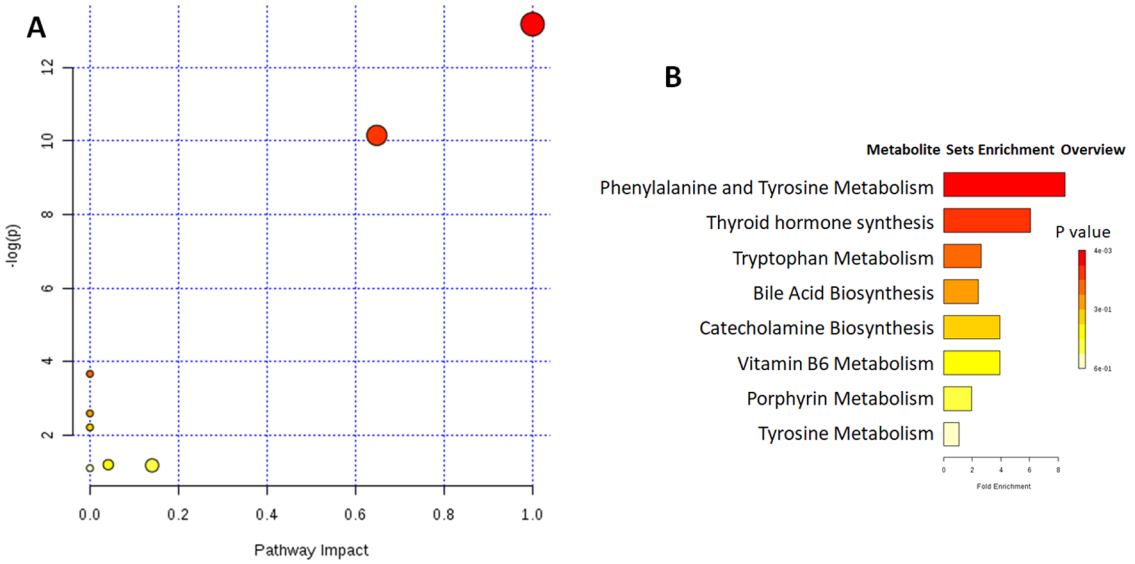

Figure 5. Metabolic pathway analysis (A) and metabolite sets' enrichment overview (B) for potential biomarkers related to the liver and kidney injury induced by PM. The most relevant pathways are represented by large and dark nodes. 1, phenylalanine and tyrosine metabolism; 2, tryptophan metabolism; 3, bile acid biosynthesis; and 4, vitamin B6 metabolism.

multivariate analysis was necessary to discern potential relationships.

To explore the changes in endogenous markers with the duration of PM administration, the OPLS-DA model was applied to confirm the potential biomarkers of liver and kidney damage caused by prolonged administration. The control group and PM groups were compared in pairs to find differences between groups. The results of the orthogonal projections to latent structures discriminant analysis (OPLS-DA) model derived from the ESI^+ and ESI^- data are displayed in Figure 3C–F.

The following clear differences were obtained: in the urine sample analysis in the positive-ion mode, the control group versus PM group I comparison had a cumulative R^2Y of 0.998 and a Q^2 of 0.952 (Figure 3G) and the control group versus PM group II comparison had an R^2Y of 0.998 and a Q^2 of 0.975 (Figure 3H); and in the urine sample analysis in the negative-ion mode, the control group versus PM group I comparison had a cumulative R^2Y of 0.976 and a Q^2 of 0.900 (Figure 3G) and the control group versus PM group II comparison had an R^2Y of 0.994 and a Q^2 of 0.972 (Figure 3H).

Potential Biomarker Selection, Discovery, and Explanation. Differential metabolites with variables with importance parameter values higher than 1 (VIP > 1) from the OPLS-DA score plots were selected for further *t*-tests and ANOVA using Progenesis QI software. Nonparametric tests were performed to identify significant differences in metabolites with $p < 0.05$ and fold change >1.5 between the control and PM groups. Differential metabolites related to the liver and kidney injury caused by PM were identified. Based on the accurate mass number, retention time, and tandem mass spectrometry (MS/MS) information of the metabolites, the metabolite ions were identified with the combination of online database information and standard sample spectra. Combined with the accurate mass-to-charge ratio in the METLIN database, HMDB database, and standard reference substances, 12 metabolites were considered as unique biomarkers for urine samples. The average normalized quantities of the 12 differential metabolites are shown in Figure 4A,B.

https://dx.doi.org/10.1021/acsomega.0c00647
ACS Omega 2020, 5, 10489−10500

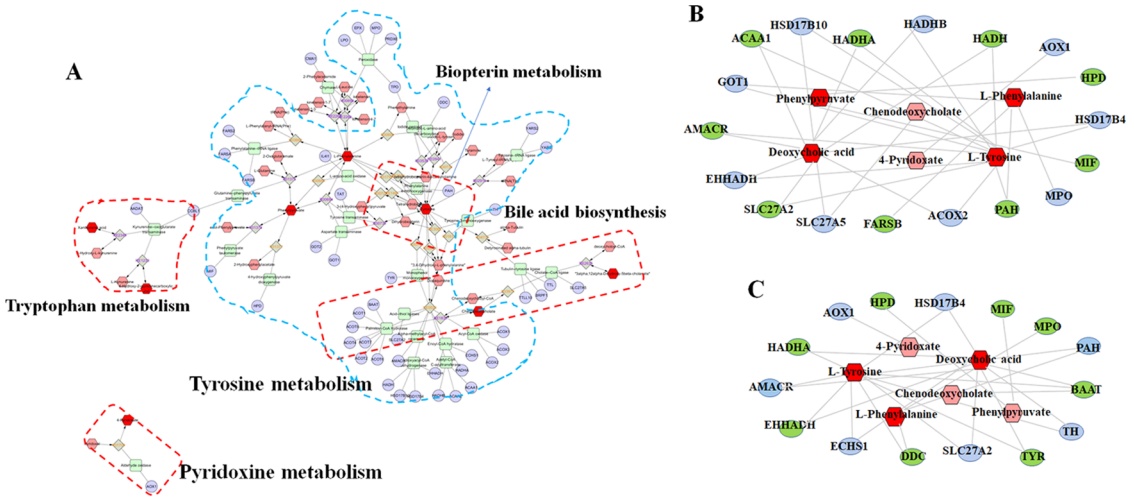

Figure 6. Metabolite−protein targets correlation. (A) Metabolic correlation network analysis. (B, C) Metabolite−potential marker correlations for toxicity induced by PM for 4 and 8 weeks, respectively. (A) Hexagon, metabolites; round rectangle, enzyme; ellipse, gene; and diamond, reaction. (The high-resolution and unprocessed (A) is shown in Figure S3.) (B, C) Metabolites and proteins are represented with (red hexagon)(pink hexagon) and (gray ellipse)(green ellipse), respectively.

Table 2. Full Names of the Potential Protein Targets[a]

targets for 4 week administration		targets for 8 week administration	
name abbreviation	full name	name abbreviation	full name
ACOX2	acyl-coenzyme A oxidase 2	TYR	tyrosinase
PAH	**phenylalanine hydroxylase**	TH	tyrosine hydroxylase
MPO	**myeloperoxidase**	BAAT	bile acid-CoA: amino acid *N*-acyltransferase
MIF	**macrophage migration inhibitory factor**	**PAH**	**phenylalanine hydroxylase**
HSD17B4	hydroxysteroid 17-β dehydrogenase 4	**MPO**	**myeloperoxidase**
HPD	**4-hydroxyphenylpyruvate dioxygenase**	**MIF**	**macrophage migration inhibitory factor**
AOX1	**aldehyde oxidase 1**	HSD17B4	hydroxysteroid 17-β dehydrogenase 4
HADH	hydroxyacyl-CoA dehydrogenase	**HPD**	**4-hydroxyphenylpyruvate dioxygenase**
HADHB	hydroxyacyl-CoA dehydrogenase trifunctional multienzyme complex subunit β	**AOX1**	**aldehyde oxidase 1**
HADHA	**hydroxyacyl-CoA dehydrogenase trifunctional multienzyme complex subunit α**	**HADHA**	**hydroxyacyl-CoA dehydrogenase trifunctional multienzyme complex subunit α**
HSD17B10	hydroxysteroid 17-β dehydrogenase 10	**AMACR**	**α-methylacyl-CoA racemase**
ACAA1	acetyl-CoA acyltransferase 1	**EHHADH**	**enoyl-CoA hydratase and 3-hydroxyacyl-CoA dehydrogenase**
GOT1	glutamic-oxaloacetic transaminase 1	ECHS1	enoyl-CoA hydratase, short chain 1
AMACR	**α-methylacyl-CoA racemase**	DDC	dopa decarboxylase
EHHADH	**enoyl-CoA hydratase and 3-hydroxyacyl-CoA dehydrogenase**	**SLC27A2**	**solute carrier family 27 member 2**
SLC27A2	**solute carrier family 27 member 2**		
SLC27A5	solute carrier family 27 member 5		
FARSB	phenylalanyl-tRNA synthetase β subunit		

[a]The targets in bold are the common targets for two time points of administration.

Biochemical Interpretation and Pathway Analysis. The changes in the concentrations of potential biomarkers (Table 1) suggested that the metabolic disturbances in rats with the liver and kidney injury, such as phenylalanine and tyrosine metabolism, were caused by the administration of PM for different durations. The most affected pathways were phenylalanine and tyrosine metabolism, tryptophan metabolism, bile acid biosynthesis, and vitamin B6 metabolism (Figure 5).

Metabolic Correlation Protein Analysis Results. As shown in Figure 6A, metabolite−protein correlation analysis was performed using Cytoscape 3.7.1. The pathways generated by Cytoscape are labeled in the figure and mainly involve tryptophan metabolism, pyridoxine metabolism, tyrosine metabolism, biopterin metabolism, and bile acid biosynthesis. In addition, potential proteins related to metabolic biomarkers were discovered. Finally, 18 proteins (ACOX2, PAH, MPO, MIF, HSD17B4, HPD, AOX1, HADH, HADHB, HADHA, HSD17B10, ACAA1, GOT1, AMACR, EHHADH, SLC27A2, SLC27A5, and FARSB) and 15 proteins (TYR, TH, BAAT, PAH, MPO, MIF, HSD17B4, HPD, AOX1, HADHA, AMACR, EHHADH, ECHS1, DDC, and SLC27A2) with full names, shown in Table 2, were considered as potential markers of toxicity induced by PM in the 4th week and 8th week, respectively. The metabolite−potential marker correlations are shown in Figure 6B,C.

https://dx.doi.org/10.1021/acsomega.0c00647
ACS Omega 2020, 5, 10489−10500

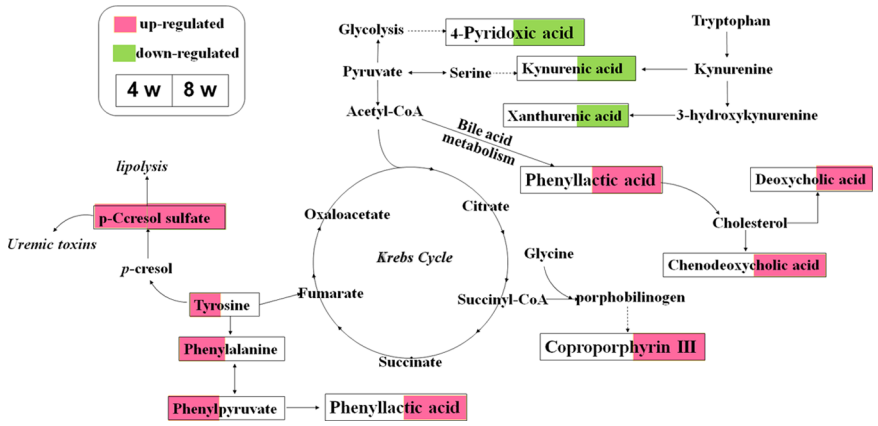

Figure 7. Perturbed metabolic pathways detected by UPLC/MS/MS analysis, showing the interrelationship between the identified metabolic pathways.

DISCUSSION

As a traditional Chinese medicine, PM has been widely used in clinical practice in China for a long time. Modern pharmacological studies have shown that PM has antitumor, antibacterial, anti-inflammatory, antioxidative, and neuroprotective activities, that it delays atherosclerosis, and that it could be used in diabetes and cardiovascular diseases.[23] The first study focused on the toxicity of PM was reported in 1996.[24] The chemical constituents of PM were anthraquinones, flavonoids, phenolic acids, stilbenes, and phospholipids. Anthraquinones in PM were ingredients of duality with toxicity and efficacy, which are related to mitochondrial abnormality, and the practical applications should be cautious. Research studies showed that chrysophanol, a naturally occurring anthraquinone that was found in PM, could be inserted into the base pair of double-stranded DNA, damaging the DNA and producing genotoxicity.[25,26] The toxic effects of emodin, such as nephrotoxicity, hepatotoxicity, genotoxicity, and reproductive toxicity, have also been reported.[27−31] Zhong et al. concluded that rhein has protective effects against acetaminophen-induced hepatic and renal toxicity in vivo experiments.[32] Aloe emodin showed a certain hepatotoxic effect by the modification of nuclear factor (NF)-κB inflammatory pathway and P53 apoptosis pathway.[33] Wang et al. evaluated the effects of representative quinone constituents of PM on UGT1A1 activity in vitro, and to examine their structure−activity relationships, they found that *cis*-emodin dianthrones, *trans*-emodin dianthrones, and emodin-8-*O*-glc showed strong inhibition of UGT1A1 and thus warrant particular attention.[34]

In recent years, many studies have reported that the long-term use of PM and its preparations showed increased hepatotoxicity, resulting in liver damage. Emodin, the main anthraquinone component of PM, induced severe cytotoxicity in the human hepatocyte line L-02 in a concentration- and time-dependent manner, while the accumulation of emodin in cells showed time-dependent cytotoxic kinetics.[35] Most PM studies have mainly focused on liver injury, but there have been a few reports on the kidney injury induced by PM. In this study, rats were treated with PM for 4 and 8 weeks and urine samples were collected at different stages for metabolomic analysis and biomarker and target prediction. Biochemical and pathological analyses of the serum and liver and kidney tissues were carried out to elucidate the mechanism of the PM-induced liver and kidney injury.

Following the state of the animals, no abnormal symptoms were observed in all of the animals after 4 weeks of PM administration. After 8 weeks of PM administration, some of the animals showed symptoms such as reduced food intake, slightly reduced body weight, decreased activity, sparse body hair, loss of luster, vertical hair, bow back curling, and so on. During the experiment, the weight of all of the animals increased slowly. With the prolongation of the PM administration time, the weight growth rate slowed down. During the experiment, the weights of all of the animals in the PM administration group were lower than those in the control group, but there was no statistical difference between the two groups (Figure S4).

Biochemical Analysis and Histopathological Change. According to biochemical indices, the synthesis and reabsorption of processes of the liver were reflected by the TBA content. After liver injury, the TBA in the intestine and kidney could not be absorbed effectively, which led to an increase in TBA.[36] Dong et al.[19] found a relationship between bile acids and liver injury in PM after 42 days of treatment. The level of TBA was found significantly increased after the 8 week administration of PM. Our previous studies have shown that PM could cause bilirubin accumulation by inhibiting uridine diphosphate (UDP)-glucuronosyltransferase 1A1 (UGT1A1) enzymes that resulted in increased bilirubin.[37] The increases in DBIL and TBIL were consistent with our studies. Changes in serum ALT, AST, and ALP are related to the extent of hepatocyte damage.[38] AST, ALT, and ALP have an upward tendency after PM administration in this study that showed some hepatocyte damage to a certain extent. The biochemical results showed that the long-term administration of PM damaged the liver by affecting the liver metabolism and probably aggravated the inhibition of UGT1A1 enzymes.

Moreover, serum BUN and creatinine, which reflect glomerular filtration function, are commonly used in the clinical evaluation of the renal function. In addition, as the final product of purine metabolism, UA is filtered through the glomeruli, reabsorbed by renal tubules, and finally discharged from the body. The level of UA increases when the renal function is abnormal.[39] In this study, compared with the control condition, 8 weeks of PM administration significantly altered BUN and UA, but there was no significant difference at 4 weeks. Although the changes were not significant at 4 and 8 weeks after PM administration, the levels of creatinine showed an increasing trend. The above results showed that no obvious

https://dx.doi.org/10.1021/acsomega.0c00647
ACS Omega 2020, 5, 10489−10500

renal damage was observed in the 4th week of PM administration, and with the increase in the length of administration to 8 weeks, the damage was significantly aggravated.

Biomarkers Obtained on the 4th and 8th Weeks of PM Administration. Li et al.[20] found that 21 potential metabolomic biomarkers that differentially expressed in the lipopolysaccharide (LPS)/ethyl acetate (EA) group compared with other groups without liver injury were identified by untargeted metabolomics. Xia et al.[40] identified 16 possible endogenous metabolites in serum by gas chromatography (GC)−MS through a nontargeted metabonomics approach and found that the mechanism of liver injury caused by PM may be related to the amino acid, fatty acid, and energy metabolism. Zhang et al.[21] identified significantly impacted biomarkers in 16 urine samples by high-performance liquid chromatography (HPLC)−MS, and the results suggested that vitamin B6 metabolism and tryptophan metabolism may be involved in the liver injury induced by PM. In our study, LC/MS-based metabonomics was used for comprehensive metabolomics analysis and provided the overall metabolites changes. According to the analysis of differential markers present after 4 weeks of PM treatment, the levels of tyrosine, L-phenylalanine, phenylpyruvate, and *p*-cresol sulfate were increased significantly (Figure 7), indicating that aromatic amino acid, phenylalanine, and tyrosine metabolism pathways were the main impacted pathways. Reduced amino acid metabolism, hepatocyte necrosis, and enhanced protein decomposition led to increased amino acid concentrations in the liver cells.[41] Tyrosine can be metabolized into phenylalanine in a reaction catalyzed by phenylalanine hydroxylase (PAH), and the lack of polycyclic aromatic hydrocarbons (PAHs) or the decline of liver activity caused the confusion of phenylalanine metabolism and acute liver injury happened.[42] As a uremic toxin, *p*-cresol sulfate in intestinal flora can be produced by the metabolism of tyrosine and phenylalanine. Besides, *p*-cresol sulfate led to nephrotoxicity and vascular toxicity[39,43] and induced stress response cells in renal tubular cells and kidney fibrosis by activating the intrarenal renal renin−angiotensin−aldosterone system (RAAS).[44] Thus, phenylalanine metabolism disorders were involved in both acute liver injury and chronic kidney injury on the 4th week of PM administration.

Kynurenic acid, xanthurenic acid, and 4-pyridoxic acid were significantly decreased, while deoxycholic acid, chenodeoxycholic acid, 12-ketodeoxycholic acid, and coproporphyrin III were significantly increased in PM group II compared with those in the control group. Kynurenic acid and xanthurenic acid are mainly involved in tryptophan metabolism, which may be as a result of their accumulation in the blood or renal insufficiency.[45] Some researchers have shown that tryptophan is closely related to liver fibrosis induced by thioacetamide.[46,47] In the tryptophan metabolism pathway, reduced levels of kynurenic acid and xanthurenic acid cause liver dysfunction.[48,49] In addition, glutathione production and abnormal vitamin B levels are both regulated by 4-pyridoxolic acid, which depends on hypersulfate reactions in methionine metabolism. As a metabolite of vitamin B6, 4-pyridoxic acid regulates glutathione production and abnormal vitamin-B-dependent hypersulfate reactions during methionine metabolism.[50] The relative concentration of 4-pyridoxic acid was significantly affected for LPS/PM extract treatment.[20] Previous studies have shown that 1 month after PM administration the disruption of vitamin B6 metabolism increased pyridoxamine levels and decreased 4-pyridoxalic acid levels in urine samples,[51,52] and these effects were also shown in our study.

Some studies have reported that PM could disturb bile and bilirubin metabolism.[19,53] The damaged liver cannot effectively reabsorb TBA into the intestinal−hepatic circulation, resulting in an increase in TBA.[54,55] Deoxycholic acid, chenodeoxycholic acid, and 12-ketodeoxycholic acid are all involved in the bile acid metabolic pathway as the predominant bile acids.[19] The amounts of these three bile acids excreted in urine through bile acid metabolism were increased sharply in our study.

In addition, bilirubin is the main metabolite of iron porphyrin in vivo. As a kind of porphyrin, coproporphyrin III enters the mitochondria, where it is oxidized and decarboxylated to form protoporphyrin IX. It is catalyzed by a ferrous-chelating enzyme, which binds Fe^{2+} to protoporphyrin IX to form heme. Drug toxicity can lead to liver damage and hemoglobin synthesis dysfunction, which increases the synergistic porphyrin III in the urine,[56] and in turn causes abnormal bilirubin metabolism and increases the level of DBIL. The content of *p*-cresol sulfate decreased significantly in PM group I compared with the control group, which indicated that the kidney was probably in the compensatory stage and could reduce the severity of damage. The metabolite *p*-cresol sulfate is produced from the amino acid phenylalanine and tyrosine by intestinal anaerobic bacteria. With the decrease of *p*-cresol sulfate in PM groups, levels of L-phenylalanine and L-tyrosine were increased.

In summary, the observed changes, which included biochemical indicators, pathological results, and biomarkers, indicated that with prolonged administration the degree of the liver injury increased and the impacted metabolic pathways changed significantly. In recent years, there were more reports about clinical adverse reactions of PM and its preparations, but at present, the components of PM leading to the liver and kidney injury were still not clear. Many contradictions of PM were reported in the publications, and the mechanism of the liver and kidney injury caused by chemical components in PM and its preparations was still not comprehensive. Moreover, during the following work, we would pay more attention to the toxicity of the main substances separated from the PM.

CONCLUSIONS

This study investigated the liver and kidney toxicity caused by PM administration by biochemical analysis, histopathological observation, and metabolomics. Biomarkers associated with PM toxicity were identified in the metabolomics study, and the corresponding targets were predicted. Metabolic pathway analysis indicated that the phenylalanine and tyrosine metabolic pathways were the main pathways affected by PM, which could cause liver damage and chronic kidney injury. With prolonged administration, the toxicity of PM gradually affected the metabolism of vitamin B6, bile acid, and bilirubin, resulting in the increased liver damage, abnormal biochemical indicators, and nephrotoxicity, which suggested that the hepatotoxicity and nephrotoxicity of PM is a dynamic process that impacts different administration times. In particular, the liver and kidney damage caused by PM should be treated differently according to different stages in the clinic.

https://dx.doi.org/10.1021/acsomega.0c00647
ACS Omega 2020, 5, 10489−10500

MATERIALS AND METHODS

Chemicals and Reagents. Chromatographic-grade methanol, acetonitrile, and formic acid were purchased from Fisher Co. (Pittsburg, PA). Purified water was prepared by a Milli-Q ultrapure water system (Millipore, Bedford, MA). The dry roots of PM were purchased from Shaanxi Jiahe Phytochem Co. Ltd. (Xi'an, Shaanxi Province, China) and authenticated by Prof. Jianrong Li (Institute of Chinese Materia Medica, China Academy of Chinese Medical Sciences). The standards L-tyrosine (no. TSN-375542), L-phenylalanine (no. PYL-091102), kynurenic acid (no. KRA-710179), chenodeoxycholic acid (no. DXC-105508), and deoxycholic acid (no. DXC-105609) were purchased from Stanford Chemicals (Lake Forest, CA).

Preparation of PM Decoction and Animal Experiments. We used cold-soaked extraction in the experiment.[14] Dried PM roots were crushed to a coarse powder, accurately weighed, immersed in 75% ethanol−water (v/v) 6 times, and extracted by refluxing at room temperature (25 °C) 5 times for 48 h each time. After the extraction finished, the five filtrates were combined, depressurized, and filter-concentrated. Then, the extract was concentrated under reduced pressure at 45 °C and dried in vacuum at 45 °C (see Figure S1 in the Supporting Information for a comprehensive description of the main components of the PM decoction). The dried powder of PM extract is added into carboxymethyl cellulose (CMC)−Na solution (0.3%) and configured as PM suspension. The weight of 20 g/kg was converted into volume for intragastric administration.

All procedures involving animals were approved by the Animal Care and Use Committee of Dongfang Hospital of Beijing University of Chinese Medicine Animal Center to ensure ethical use and humane treatment of the animals. Thirty adult male Sprague−Dawley rats, specific pathogen-free (SPF) grade, weighing 220−250 g, were provided by Beijing Vital River Laboratory Animal Technology Co., Ltd. with the permission number SCXK (JING) 2016-006. All animals were kept in a laboratory animal room at 25 °C under a 12 h light/dark cycle and 45 ± 5% humidity with free access to water and standard laboratory chow. The rats were divided randomly into three groups: the control group, in which ten rats were orally administered with an equivalent volume of solvent (0.3% CMC−Na); PM group I (for 4 weeks), in which ten rats were administrated orally with 20 g/kg[14] PM suspension once a day for 4 weeks (measured as the quantity of the crude material); and PM group II (for 8 weeks), in which ten rats were administrated orally with 20 g/kg PM suspension once a day for 8 weeks (measured as the quantity of the crude material).

Collection and Handling of Animal Samples. After 4 weeks, each rat in PM group I was placed in a single metabolic cage to collect urine for 24 h. Twelve hours after the last administration, the rats were anesthetized with sodium pentobarbital (50 mg/kg, i.p.). The blood samples of the rats were collected from the abdominal aorta with a syringe. Then, the blood samples were centrifuged at 3500*g* for 10 min and the supernatant serum was transferred into a clean plastic tube for blood biochemical analysis

After the rats were euthanized by exsanguination, the liver and kidney tissues were immediately removed from the rats for histopathological analysis.

Similarly, after 8 weeks, each rat in the control group and PM group II was placed in single metabolic cages to collect urine for 24 h. The rats in these groups underwent the same procedure as those in PM group I.

Serum Biochemistry and Histopathological Analysis. Serum hepatotoxicity index (including ALT, AST, ALP, TBA, TBIL, and DBIL) and nephrotoxicity index (including BUN, Crea, UA, and β2-microglobulin (β2-MG)) levels were measured using a Hitachi 17080 automatic biochemistry analyzer (Tokyo, Japan). The liver and kidney tissues to be used for histopathological examination were placed in 4% paraformaldehyde. The tissues were then further processed, embedded in paraffin, and stained with hematoxylin and eosin.

Urine Sample Handling for Metabolomics Analysis. Prior to analysis, 200 μL of aliquots of urine samples were thawed at 4 °C followed by the addition of 800 μL methanol to precipitate the proteins, according to the method of Shoubei Qi et al. The resulting solution mixture was vortexed for 30 s and centrifuged at 13 000 rpm for 15 min at 4 °C. The supernatant (800 μL of urine for each sample) was transferred to an Eppendorf (EP) tube and evaporated to dryness at 36 °C under a stream of nitrogen. The residue was dissolved in 100 μL of methanol followed by vertexing for 60 s and centrifuging at 13 000 rpm for 15 min. The clear supernatant (50 μL) was transferred to a sampling vial for ultraperformance liquid chromatography−quadrupole-time-of-flight mass spectrometry (UPLC−Q-TOF-MS) analysis. A quality control sample was prepared by pooling aliquots from all samples collected in the course of the study.

Chromatography and MS Conditions. Waters Synapt G2 (Waters Corporation, Milford, MA) was used for UPLC−Q-TOF-MS. Chromatographic separation was performed at 40 °C on an Acquity UPLC HSS C_{18} column (1.7 μm, 2.1 × 100 mm^2). The mobile phase consisted of 0.1% formic acid−water (A) and 0.1% formic acid−acetonitrile (B). The UPLC elution conditions are as follows: 0−1.5 min, 10−20% B; 1.5−4 min, 20−40% B; 4−13 min, 40−90% B; 13.1−14 min, 90% B; and 14.1−17 min, 10% B. The flow rate was set to 0.4 mL/min, and the injection volume was 4 μL. The autosampler was maintained at 10 °C. Using the TOF-MS model, the electrospray ionization (ESI) source was operated in both positive and negative modes. Accurate mass determination using leucine−enkephalin (ESI^+, m/z 556.2771; ESI^-, m/z 554.2615) was used to lock the mass solution. The parameters in the positive-ion detection mode are as follows: capillary voltage, 2.7 kV; source temperature, 120 °C; desolvation temperature, 500 °C; cone gas flow, 50 L/h; desolvation gas flow, 800 L/h; and collision energy, 25−50 eV. The negative-ion detection mode was the same as the positive-ion detection mode, except for being negative in the capillary voltage 2.1 kV. The mass spectrum was collected in the profile mode ranging from 50 to 1000 m/z.

Data Processing and Pattern Recognition Analysis. The MS data were exported to data format (centroid) files by Masslynx Software version 4.0 (Waters Corporation). Data pretreatment procedures, such as nonlinear retention time alignment, peak discrimination, filtering, alignment, matching, and identification, were performed in Progenesis QI (Milford MA), and the retention time and mass-to-ratio data pairs were used as the parameters for each ion. The data were processed by unit variance scaling and the mean-centered method, followed by multivariate analysis, including PCA. A permutation test was used to prevent overfitting of the OPLS-DA model. VIP > 1 in the OPLS-DA model was selected as the potential variable. Meanwhile, Progenesis QI software was

https://dx.doi.org/10.1021/acsomega.0c00647
ACS Omega 2020, 5, 10489−10500

used to perform Student's *t*-test and one-way analysis of variance (ANOVA) for these variables. Metabolites with $p < 0.05$ (ANOVA and *t*-test) and fold change >2 were considered to be statistically significant.

Biomarker Identification and Metabolic Pathway Analysis. Ions were verified based on the extracted ion chromatogram in the raw MS data. Accurate masses of quasi-molecular ions were put into online databases, such as the Human Metabolome Database (http://www.hmdb.ca/), METLIN (http://metlin.scripps.edu), and SMPD (http://www.smpdb.ca/), to identify possible metabolites. In the next step, the spectra were compared with the MS/MS information from the above databases in Waters Mass Fragment software to verify the structure of the putative metabolites. Finally, the metabolites were identified by comparing the retention times and fragments of metabolites with those of reference samples. The pathways of potential biomarkers were analyzed using MetaboAnalyst 3.0 (http://www.metaboanalyst.ca/). *Rattus norvegicus* in the pathway path library was selected for pathway enrichment and topological analysis, and the other parameters were set at the default level.

Metabolic Correlation Protein Analysis. Cytoscape 3.7.1 and GeneCards (https://www.genecards.org/) were used for the metabolic correlation protein analysis and to obtain potential protein targets of PM toxicity. Pathways closely related to potential biomarkers were explored and further discussed. Proteins targets related to biomarkers were identified with Cytoscape, and the potential protein targets were predicted with GeneCards.

■ ASSOCIATED CONTENT

Supporting Information

The Supporting Information is available free of charge at https://pubs.acs.org/doi/10.1021/acsomega.0c00647.

UPLC−Q-TOF-MS characteristic chromatogram of decoction of PM (Figure S1); representative BPI chromatograms from the positive and negative ions in urine samples (A, positive; B, negative) (Figure S2); metabolite−protein target correlation (Figure S3); and animals weight ($n = 10$) (Figure S4) (PDF)

■ AUTHOR INFORMATION

Corresponding Authors

Binyu Wen − *Dongfang Hospital, Beijing University of Chinese Medicine, Beijing 100078, P. R. China*; Email: wen-binyu@163.com

Jian Gao − *Beijing University of Chinese Medicine, Beijing 100078, P. R. China*; orcid.org/0000-0003-0959-5509; Email: gaojian_5643@163.com

Authors

Yan Yan − *Dongfang Hospital, Beijing University of Chinese Medicine, Beijing 100078, P. R. China*

Ning Shi − *Pharmaceutical Department of Characteristic Medical Center, Strategic Support Force, Beijing 100101, P. R. China*

Xuyang Han − *Beijing Institute of Traditional Chinese Medicine, Beijing Hospital of Traditional Chinese Medicine, Capital Medical University, Beijing 100010, P. R. China*

Guodong Li − *Beijing University of Chinese Medicine, Beijing 100078, P. R. China*

Complete contact information is available at: https://pubs.acs.org/10.1021/acsomega.0c00647

Author Contributions

#Y.Y. and N.S. contributed equally to this work; B.W. and J.G. conceived and designed the experiments; Y.Y. and N.S. performed the experiments; X.H. and G.L. analyzed the data; and B.W. and J.G. wrote and revised the manuscript. All authors read and approved the final manuscript.

Funding

This work was supported by the Fundamental Research Funds for the Central Universities (no. 2018-JYBZZ-JS104), the Exploratory Project of Basic Medical and Health Research of Characteristic Medical Center of Strategic Support Force (no. 19ZX63), and the China Postdoctoral Science Foundation (2018M641286). The Fundamental Research Fund for the Central Universities is the special fund set up by the state to support the central colleges and universities to carry out independent innovation research in the fields of basic, cross-cutting, and cutting-edge and for the cultivation of major topics and independent research. The Exploratory Project of Basic Medical and Health Research of Characteristic Medical Center of Strategic Support Force is a fundamental research fund set up by the Center to support the basic scientific issues in disease prevention and treatment and to target the structure, function, development, genetic, and immune abnormalities and diseases of the body.

Notes

The authors declare no competing financial interest.

The experimental protocols were approved by the Institutional Animal Care and Use Committee of Dongfang Hospital of Beijing University of Chinese Medicine Animal Center.

The data used to support the findings of this study are included within the article and the Supporting Information file.

■ REFERENCES

(1) Yang, Q.; Li, X. Y.; Zhao, X. M.; Sun, R. System analysis on adverse drug reaction of Chinese patent medicine containing *Polygoni Multiflori Radix*. *Chin. Tradit. Herb. Drugs* **2017**, *48*, 1878−1887.

(2) Lin, L.; Ni, B.; Lin, H.; Zhang, M.; Yan, L.; Qu, C.; Ni, J. Simultaneous determination of 14 constituents of *Radix polygoni multiflori* from different geographical areas by liquid chromatography-tandem mass spectrometry. *Biomed. Chromatogr.* **2015**, *29*, 1048−1055.

(3) Lin, L.; Ni, B.; Lin, H.; Zhang, M.; Li, X.; Yin, X.; Qu, C.; Ni, J. Traditional usages.; botany.; phytochemistry.; pharmacology and toxicology of *Polygonum multiflorum* Thunb., a review. *J. Ethnopharmacol.* **2015**, *159*, 158−183.

(4) Ip, S. P.; Tse, A. S. M.; Poon, M. K. T.; Ko, K. M.; Ma, C. Y. Antioxidant activities of *Polygonum multiflorum* Thunb., *in vivo* and *in vitro*. *Phytother. Res.* **1997**, *11*, 42−44.

(5) Li, D. P.; Zhang, N. S.; Cao, Y. G.; Zhang, W.; Su, G. L.; Sun, Y.; Liu, Z. C.; Li, F. Y.; Liang, D. J.; Liu, B.; Guo, M. Y.; Fu, Y. H.; Zhang, X. C.; Yang, Z. T. Emodin ameliorates lipopolysaccharide-induced mastitis in mice by inhibiting activation of NF-kB and MAPKs signal pathways. *Eur. J. Pharmacol.* **2013**, *705*, 79−85.

(6) Liu, M. H.; Jing, X. B.; Cai, X. B.; Chen, S. Z.; Cai, J. Y. The mechanism about the inhibition effects of emodin on the proliferation of EC-109 cell in esophageal cancer. *J. Shantou Univ. Med. Coll.* **2009**, *22*, 12−14.

(7) Ruan, L. Y.; Li, M. H.; Xing, Y. X.; Hong, W.; Chen, C.; Chen, J. F.; Xu, H.; Zhao, W. L.; Wang, J. S. Hepatotoxicity and hepatoprotection of *Polygonum multiflorum* Thund. as two sides of the same biological coin. *J. Ethnopharmacol.* **2019**, *230*, 81−94.

(8) Jung, K. A.; Min, H. J.; Yoo, S. S.; Kim, H. J.; Choi, S. N.; Ha, C. Y.; Kim, H. J.; Kim, T. H.; Jung, W. T.; Lee, O. J.; Lee, J. S.; Shim, S.

G. Drug-Induced Liver Injury, Twenty Five Cases of Acute Hepatitis Following Ingestion of *Polygonum multiflorum* Thunb. *Gut Liver* **2011**, *5*, 493−499.
(9) Dong, H.; Slain, D.; Cheng, J.; Ma, W.; Liang, W. Eighteen cases of liver injury following ingestion of *Polygonum multiflorum*. *Complementary Ther. Med.* **2014**, *22*, 70−74.
(10) Lei, X.; Chen, J.; Ren, J.; Li, Y.; Zhai, J.; Mu, W.; Zhang, L.; Zheng, W.; Tian, G.; Shang, H. Liver Damage Associated with *Polygonum multiflorum* Thunb., A Systematic Review of Case Reports and Case Series. *Evidence-Based Complementary Altern. Med.* **2015**, *2015*, No. 459749.
(11) Luo, Y. Y.; Liu, J. X.; Wang, F.; Liu, X. H.; Wang, S. N.; Hua, Y. J.; Lan, C. W.; Xing, Q. Q. Dynamic changes of metabolite accumulation of *Polygoni multifori radix* based on UPLC-Triple TOF-MS/MS. *Chin. Tradit. Herb. Drugs* **2017**, *48*, 2105−2110.
(12) Li, D. D.; Tang, X. L.; Long, L.; Xu, L. L.; Tan, H. L.; Liang, Q. D.; Xiao, C. R.; Wang, Y.; Ma, Z. C.; Wang, L. L.; Gao, Y. High-content screen assay for studying hepatotoxicity mechanisms of ethanol extract of *radix polygoni multiflori* and *radix polygoni multiflori* praeparata. *Chin. J. Pharmacol. Toxicol.* **2017**, *31*, 626−635.
(13) Huang, C. L.; Fan, X. M.; Qian, L. I.; Wang, Y. M.; Wang, S. M.; Gong, M. J.; Luo, G. A. Effect of processed *Polygonum multiflorum* on mRNA expression level of five subtypes of CYP450 enzymes in rat liver. *Zhongguo Zhongyao Zazhi* **2017**, *42*, 352.
(14) Hezhi, L. I.; Siming, D.; Xi, W.; Yang, L. Effects of *Polygonum multiflorum* on kidney injury and renal cell apoptosis in SD rats. *Chin. J. Comp. Med.* **2018**, DOI: 10.3969/j.issn.1671-7856.2018.05.015.
(15) Wang, J. B.; Ma, Y. G.; Zhang, P.; in, C.; Sun, Y. Q.; Xiao, X. H.; Zhao, Y. L.; Zhou, C. P. Effect of processing on the chemical contents and hepatic and renal toxicity of rhubarb studied by canonical correlation analysis. *Acta Pharm. Sin.* **2009**, *44*, 885−890.
(16) Zhang, L.; Li, Y.; Lin, X.; Jia, C.; Yu, X. Liquid Chromatography/Mass Spectrometry based serum metabolomics study on recurrent abortion women with antiphospholipid syndrome. *PLoS One* **2019**, *14*, No. e0225463.
(17) Cui, L.; Lu, H.; Lee, Y. H. Challenges and emergent solutions for LC-MS/MS based untargeted metabolomics in diseases. *Mass. Spectrom. Rev.* **2018**, *37*, 772−792.
(18) Yuan, M.; Kremer, D. M.; Huang, H.; Breitkopf, S. B.; Ben-Sahra, I.; Manning, B. D.; Lyssiotis, C. A.; Asara, J. M. Ex vivo and in vivo stable isotope labelling of central carbon metabolism and related pathways with analysis by LC-MS/MS. *Nat. Protoc.* **2019**, *14*, 313−330.
(19) Dong, Q.; Li, N.; Li, Q.; Zhang, C. E.; Feng, W. W.; Li, G. Q.; Li, R. Y.; Tu, C.; Han, X.; Bai, Z. F.; Zhang, Y. M.; Niu, M.; Ma, Z. J.; Xiao, X. H.; Wang, J. B. Screening for biomarkers of liver injury induced by *Polygonum multiflorum*, a targeted metabolomic study. *Front. Pharmacol.* **2015**, *6*, No. 217.
(20) Li, C.-Y.; Tu, C.; Gao, D.; Wang, R.-L.; Zhang, H.-Z.; Niu, M.; Li, R.-Y.; Zhang, C.-E.; Li, R.-S.; Xiao, X.-H.; et al. Metabolomic Study on Idiosyncratic Liver Injury Induced by Different Extracts of *Polygonum multiflorum* in Rats Integrated with Pattern Recognition and Enriched Pathways Analysis. *Front. Pharmacol.* **2016**, *7*, No. 483.
(21) Zhang, C. E.; Niu, M.; Li, Q.; Zhao, Y.-l.; Ma, Z.-j.; Xiong, Y.; Dong, X.-p.; Li, R.-y.; Feng, W.-w.; Dong, Q.; et al. Urine metabolomics study on the liver injury in rats induced by raw and processed *Polygonum multiflorum* integrated with pattern recognition and pathways analysis. *J. Ethnopharmacol.* **2016**, *194*, 299−306.
(22) Perera, T.; Ranasinghe, S.; Alles, N.; Waduge, R. Effect of fluoride on major organs with the different time of exposure in rats. *Environ. Health Prev. Med.* **2018**, *23*, No. 17.
(23) He, D. X.; Chen, B.; Tian, Q.; Yao, S. Simultaneous determination of five anthraquinones in medicinal plants and pharmaceutical preparations by HPLC with fluorescence detection. *J. Pharm. Biomed. Anal.* **2009**, *49*, 1123−1127.
(24) But, P. P.; Tomlinson, B.; Lee, K. L. Hepatitis related to the Chinese medicine Shou-wu-pian manufactured from *Polygonum multiflorum*. *Vet. Hum. Toxicol.* **1996**, *38*, 280−282.
(25) Yang, X. M.; Li, J. S.; Huang, G. X.; Li, Q. Q.; Yan, L. J. Study on potential toxic mechanism of chrysophanol binding DNA by saturation value binding DNA. *Asian J. Chem.* **2012**, *24*, 551−557.
(26) Yang, X. M.; Li, J. S.; Li, Q. Q.; Huang, G. X.; Yan, L. J. Evaluation of the potential toxicity of anthraquinone derivatives in Chinese herbal medicines by the resonance light scattering spectrum. *Asian J. Chem.* **2011**, *23*, 3631−3634.
(27) Wang, C.; et al. Emodin induces apoptosis through caspase 3-dependent pathway in HK-2 cells. *Toxicology* **2007**, *231*, 120−128.
(28) Wang, Q-x.; Wu, C.-q.; Yang, H.-l.; Jing, S.-f.; Jin, C.; Xiao, X.-h.; Liao, M.-y. Cytotoxicity of free anthraquinone from Radix et Rhizoma Rhei to HK-2 Cells. *Chin. J. New Drugs* **2007**, *16*, 189.
(29) Cui, C.-L.; Ma, J.; Zheng, L.; Li, H.-J.; Li, P. Determination of emodin in L-02 cells and cell culture media with liquid chromatographymass spectrometry, application to a cellular toxicokinetic study. *J. Pharm. Biomed. Anal.* **2012**, *71*, 71−78.
(30) Peng, C.; Wang, Y.; Li, Y. Toxicity mechanism of emodin on interstitial cells of Cajal. *Pharmacol. Pharm.* **2013**, *4*, 331−339.
(31) Luo, T.; Li, N.; He, Y. Q.; Weng, S. Q.; Wang, T.; Zou, Q. X.; Zeng, X. H. Emodin inhibits human sperm functions by reducing sperm $[Ca^{2+}]_i$ and tyrosine phosphorylation. *Reprod. Toxicol.* **2015**, *51*, 14−21.
(32) Zhong, X. F.; Huang, G. D.; Luo, T.; Deng, Z. Y.; Hu, J. N. Protective effect of rhein against oxidative stress-related endothelial cell injury. *Mol. Med. Rep.* **2012**, *5*, 1261−1266.
(33) Quan, Y.; Gong, L.; He, J.; Zhou, Y.; Liu, M.; Cao, Z.; Li, Y.; Peng, C. Aloe emodin induces hepatotoxicity by activating NF-κB inflammatory pathway and P53 apoptosis pathway in zebrafish. *Toxicol. Lett.* **2019**, *306*, 66−79.
(34) Wang, Q.; Wang, Y.; Li, Y.; Wen, B.; Dai, Z.; Ma, S.; Zhang, Y. Identification and characterization of the structure−activity relationships involved in UGT1A1 inhibition by anthraquinone and dianthrone constituents of *Polygonum multiflorum*. *Sci Rep.* **2017**, *7*, No. 17952.
(35) Li, C. L.; Ma, J.; Zheng, L.; Li, H. J.; Li, P. Determination of emodin in L-02 cells and cell culture media with liquid chromatography-mass spectrometry, Application to a cellular toxicokinetic study. *J. Pharm. Biomed. Anal.* **2012**, *71*, 71−78.
(36) Ferslew, B. C.; Xie, G.; Johnston, C. K.; Su, M.; Stewart, P. W.; Jia, W.; Brouwer, K. L.; Barritt, A. S. Altered Bile Acid Metabolome in Patients with Nonalcoholic Steatohepatitis. *Dig. Dis. Sci.* **2015**, *60*, 3318−3328.
(37) Wang, Q.; Dai, Z.; Wen, B.; Ma, S.; Zhang, Y. Estimating the Differences of UGT1A1 Activity in Recombinant UGT1A1 Enzyme.; Human Liver Microsomes and Rat Liver Microsome Incubation Systems in Vitro. *Biol. Pharm. Bull.* **2015**, *38*, 1910−1917.
(38) Penndorf, V.; Saner, F.; Gerken, G.; Canbay, A. Liver parameters in intensive care medicine. *Zentralbl. Chir.* **2013**, *138*, 636−642.
(39) Raff, A. C.; Meyer, T. W.; Hostetter, T. H. New insights into uremic toxicity. *Curr. Opin. Nephrol. Hypertens.* **2008**, *17*, 560−565.
(40) Xia, X. H.; Yuan, Y. Y.; Liu, M. The assessment of the chronic hepatotoxicity induced by.; *Polygoni Multiflori.; Radix* in rats, A pilot study by using untargeted metabolomics method. *J. Ethnopharmacol.* **2017**, *203*, 182−190.
(41) An, Z. L.; Shi, C.; Zhao, R.; Li, P. F.; Liu, L. H. Ultra High Performance Liquid Chromatography Coupled with Q Exactive Hybrid Quadrupole-orbitrap Mass Spectrometry for Serumal Metabonomics Study of Drug-induced Liver Injury in Patients. *Chin. J. Anal. Chem.* **2015**, *43*, 1408−1414.
(42) Valdivieso, F.; Gimenez, C.; Mayor, F. In vivo inhibition of rat liver phenylalanine hydroxylase by p-chlorophenylalanine and Esculin. Experimental model of phenylketonuria. *Biochem. Med.* **1975**, *12*, 72−78.
(43) Gironès, N.; Carbajosa, S.; Guerrero, N. A.; Poveda, C.; Chillón-Marinas, C.; Fresno, M. Global metabolomic profiling of acute myocarditis caused by *Trypanosoma cruzi* infection. *PLoS Neglected Trop. Dis.* **2014**, *8*, No. e3337.

(44) Sun, C. Y.; Chang, S. C.; Wu, M. S. Uremic Toxins Induce Kidney Fibrosis by Activating Intrarenal Renin-Angiotensin-Aldosterone System Associated Epithelial-to-Mesenchymal Transition. *PLoS One* **2012**, *7*, No. e34026.
(45) Pawlak, D.; Tankiewicz, A.; Buczko, W. Kynurenine and its metabolites in the rat with experimental renal insufficiency. *J. Physiol. Pharmacol.* **2001**, *52*, 755−766.
(46) Wei, D. D.; Wang, J. S.; Wang, P. R.; Li, M. H.; Yang, M. H.; Kong, L. Y. Toxic effects of chronic low-dose exposure of thioacetamide on rats based on NMR metabolic profiling. *J. Pharm. Biomed. Anal.* **2014**, *98*, 334−338.
(47) An, Z.; Li, C.; Lv, Y.; Li, P.; Wu, C.; Liu, L. Metabolomics of Hydrazine-Induced Hepatotoxicity in Rats for Discovering Potential Biomarkers. *Dis. Markers* **2018**, *2018*, No. 8473161.
(48) Rios-Avila, L.; Nijhout, H. F.; Reed, M. C.; Sitren, H. S.; Gregory, J. F. A mathematical model of tryptophan metabolism via the kynurenine pathway provides insights into the effects of vitamin B-6 deficiency.; tryptophan loading.; and induction of tryptophan 2.;3-dioxygenase on tryptophan metabolites. *J. Nutr.* **2013**, *143*, 1509−1519.
(49) Sun, X.; Xu, W.; Zeng, Y.; Hou, Y.; Guo, L.; Zhao, X.; Sun, C. Metabonomics evaluation of urine from rats administered with phorate under long-term and low-level exposure by ultra-performance liquid chromatography-mass spectrometry. *J. Appl. Toxicol.* **2014**, *34*, 176−183.
(50) Halsted, C. H. B-Vitamin dependent methionine metabolism and alcoholic liver disease. *Clin. Chem. Lab. Med.* **2013**, *51*, 457−465.
(51) Anand, S. S. Protective effect of vitamin B6 in chromium-induced oxidative stress in liver. *J. Appl. Toxicol.* **2005**, *25*, 440−443.
(52) Mitchell, D.; Wagner, C.; Stone, W. J.; Wilkinson, G. R.; Schenker, S. Abnormal regulation of plasma pyridoxal 5′-phosphate in patients with liver disease. *Gastroenterology* **1976**, *71*, 1043−1049.
(53) Yamazaki, M.; Miyake, M.; Sato, H.; Masutomi, N.; Tsutsui, N.; Adam, K. P.; Alexander, D. C.; Lawton, K. A.; Milburn, M. V.; Ryals, J. A.; et al. Perturbation of bile acid homeostasis is an early pathogenesis event of drug induced liver injury in rats. *Toxicol. Appl. Pharmacol.* **2013**, *268*, 79−89.
(54) Lina, L.; Shelli, S.; Christopher, H.; Jiri, A.; Colangelo, J. L. Evaluation of serum bile acid profiles as biomarkers of liver injury in rodents. *Toxicol. Sci.* **2013**, *137*, 12.
(55) Masubuchi, N.; Nishiya, T.; Imaoka, M.; Mizumaki, K.; Okazaki, O. Promising toxicological biomarkers for the diagnosis of liver injury types, Bile acid metabolic profiles and oxidative stress marker as screening tools in drug development. *Chem. Biol. Interact.* **2016**, *255*, 74−82.
(56) Racz, W. J.; Marks, G. S. Drug-induced porphyrin biosynthesis. IV. Investigation of the differences in response of isolated liver cells and the liver of the intact chick embryo to porphyria-inducing drugs. *Biochem. Pharmacol.* **1972**, *21*, 143−151.

https://dx.doi.org/10.1021/acsomega.0c00647
ACS Omega 2020, 5, 10489−10500